

Phosphoproteome Reveals the Lactation Mechanism in Caprine Mammary Gland Tissues in Peak and Late Lactation Stages

Chao Zhu

Northwest Agriculture and Forestry University

Hao Yin

Northwest Agriculture and Forestry University

Quyu Duan

Northwest Agriculture and Forestry University

Fu Li

Northwest Agriculture and Forestry University

Yue Jiang

Northwest Agriculture and Forestry University

Junru Zhu

Northwest Agriculture and Forestry University

Yonglong He

Northwest Agriculture and Forestry University

Wenfei Li

Northwest Agriculture and Forestry University

Zhanhang Wang

Northwest Agriculture and Forestry University

Xiaopeng An (✉ axpdky@nwafu.edu.cn)

Northwest Agriculture and Forestry University

Research article

Keywords: phosphoproteome, lactation, IRS1, β -casein, triglycerides, goat

Posted Date: September 8th, 2020

DOI: <https://doi.org/10.21203/rs.3.rs-45445/v1>

License:   This work is licensed under a Creative Commons Attribution 4.0 International License.

[Read Full License](#)

Abstract

Background: Protein phosphorylation plays an important role in lactation. Differentially modified modification sites between peak lactation (PL, 90 days postpartum) and late lactation (LL, 280 days postpartum) were investigated using an integrated approach, namely, liquid chromatography with tandem mass spectrometry (LC-MS/MS) and tandem mass tag (TMT) labelling, to understand the molecular biological mechanisms in goat breast tissues.

Results: A total of 1,938 (1,111 up-regulated, 827 down-regulated) differentially modified modification sites of 1,172 proteins were identified (P values < 0.05 and fold change of phosphorylation ratios > 1.5). In addition, the Kyoto Encyclopedia of Genes and Genomes (KEGG) enrichment analysis showed that ribosome (chx03010), RNA transport (chx03013), protein export (chx03060), calcium signalling pathway (chx04020), oxytocin signalling pathway (chx04921), RNA degradation (chx03018) and MAPK signalling pathway (chx04010) were enriched in relation to energy metabolism and protein translation. The results of western blot showed phosphorylation levels of ACACA, EIF4EBP1 and IRS1 increased and JUN decreased in PL compared with LL. The result was consistent with phosphoproteome.

Conclusions: Overall, these data indicate that protein phosphorylation is closely related to lactation and differentially modified modification sites might have potential research value in the regulation of goat lactation.

Background

Phosphorylation is one of the important post-translational modifications of proteins; it is related to many activities of life, such as signal transduction, gene expression, cell cycle and cell apoptosis[1].

Esterification takes place as the side chain of protein amino acid is added to a phosphoric acid group with a strong negative charge, thereby changing the structure, activity and ability to interact with other molecules, affecting many biological processes. In eukaryotes, phosphorylation occurs primarily in serine, threonine and tyrosine[2].

Goat milk is very popular with the improvement of people's living conditions and the unique nutritional and health value of goat milk. Therefore, improving milk production and quality of dairy goat is the focus of our work. Dynamic changes in protein phosphorylation occur in goat mammary epithelial cells during PL period and LL period[3, 4]. Studies have shown that protein phosphorylation regulates lactation in animals[5, 6]. Although phosphoproteome analysis was conducted on the oocyte of goat[7] and the heart, liver of mice[8, 9], phosphorylated proteomic analysis has not been performed in PL and LL stages of dairy goat mammary gland tissues. The regulation mechanism of phosphorylation protein to lactation synthesis is not well known.

Therefore, in this experiment, differentially modified modification sites of phosphorylated protein between PL and LL in goat breast tissues are identified by tandem mass tag (TMT)/isobaric tags for relative and absolute quantitation (iTRAQ) labelling, high-performance liquid chromatography (HPLC) fractionation,

affinity enrichment and liquid chromatography with tandem mass spectrometry (LC–MS/MS) analysis. A total of 1,938 (1,111 up-regulated, 827 down-regulated) differentially modified modification sites of 1,172 proteins were identified and further explore the Gene Ontology (GO) and Kyoto Encyclopedia of Genes (KEGG) for differentially phosphorylated proteins. Phosphorylation levels of ACACA, EIF4EBP1, IRS1 increased and JUN decreased in PL compared with LL, the data showed that the results of phosphoproteome were reliable. The present study provided essential information to enhance the knowledge of expression dynamics of phosphorylated proteins during PL and LL and good reference data for further studying effect of protein phosphorylation to lactation in the mammary gland.

Results

Sample repeatability test and mass spectrometry quality control detection

Differentially modified modification sites were analysed by LC–MS/MS and TMT between PL and LL of goat. The workflow of the present study is shown in Fig. 1a. The results of the sample repeatability test are shown in Fig. 1b. Figure 1b is a thermal chart drawn by calculating Pearson's Correlation Coefficient between two pairs of samples. Pearson's Correlation Coefficient showed that the reproducibility of the sample was good. The mass error was detected at 0 as the centre axis and concentrated in the range of less than 10 ppm. The length of most peptide segments was between 8 and 20 amino acid residues, which indicated that the preparation of the sample was standard in our study (Fig.S1).

Analysis of differentially phosphorylated proteins

A quantitative study of differentially modified modification sites was performed in this experiment by an integrated approach involving LC–MS/MS and TMT labelling. All samples were prepared in triplicate. A total of 6,979 phosphorylation sites were identified on 2,608 proteins, of which 5,901 phosphorylation sites of 2,454 proteins contained quantitative information. In the classified groups, the variation of the difference expressed was more than 1.5 times and less than 0.67 times the change criterion of significant up-regulation or significant down-regulation (P values < 0.05). A total of 1,938 (1,111 up-regulated and 827 down-regulated) differentially modified modification sites of 1,172 proteins were changed (Fig. 2; Table S1).

To understand the phosphorylated proteins that were identified and quantified, such phosphorylated proteins and differentially modified modification sites were annotated in detail from the aspects of GO, protein domain, KEGG pathways and subcellular localisation (Table S2). To calculate the rule of amino acid sequence in the differentially modified modification sites, the amino acid sequence was detected before and after all phosphorylation sites in the samples. The results revealed that most quantified phosphorylated proteins had remarkable enrichment near the modifier sites (Fig.S2, Table S3).

A total of 2,454 proteins that contained quantitative information were classified by GO annotation based on three categories, namely, biological process, cellular component and molecular function. In the biological process type, 'cellular process' contained 160 up-regulated phosphorylated proteins (25%) and

102 down-regulated phosphorylated proteins (22%); 'metabolic process' contained 133 up-regulated phosphorylated proteins (21%) and 66 down-regulated phosphorylated proteins (15%); 'biological regulation' contained 100 up-regulated phosphorylated proteins (16%) and 86 down-regulated phosphorylated proteins (19%); 'single-organism process' contained 95 up-regulated phosphorylated proteins (15%) and 71 down-regulated phosphorylated proteins (16%). In the cellular type, 'cell' contained 115 up-regulated phosphorylated proteins (36%) and 71 down-regulated phosphorylated proteins (38%); 'organelle' contained 84 up-regulated phosphorylated proteins (26%) and 46 down-regulated phosphorylated proteins (25%); 'membrane' contained 71 up-regulated phosphorylated proteins (22%) and 32 down-regulated phosphorylated proteins (17%). In the molecular function, 'binding' contained 433 up-regulated phosphorylated proteins (68%) and 246 down-regulated phosphorylated proteins (63%); 'catalytic activity' contained 135 up-regulated phosphorylated proteins (21%) and 70 down-regulated phosphorylated proteins (18%); 'molecular function regulator' contained 30 up-regulated phosphorylated proteins (5%) and 26 down-regulated phosphorylated proteins (7%) (Fig. 3, Table S4). In addition, the subcellular localisation of proteins that contained differentially modified modification sites was predicted by wolfpsort. These proteins were assigned to 10 subcellular components, including 396 nucleus-localised proteins (54%) and 128 cytoplasm-localised proteins (17%) in the up-regulated phosphorylated proteins and 229 nucleus-localised proteins (52%) and 90 cytoplasm-localised proteins (21%) in the down-regulated phosphorylated proteins (Fig. 4, Table S5).

Functional enrichment of differentially phosphorylated proteins

Proteins that contained differentially modified modification sites were analysed by GO enrichment analysis. From the analysis of the results, up-regulated phosphorylated site corresponding proteins were primarily enriched to biological processes related to protein translation and energy metabolism, such as 'translation', 'organic substance transport', 'protein localisation' and 'Golgi vesicle transport'. For molecular function, up-regulated phosphorylated sites corresponding proteins were primarily enriched to 'transporter activity' and 'structural constituent of ribosome', which were also related to translation and transportation. Similarly, up-regulated phosphorylated sites corresponding proteins were primarily enriched to organelles related to translation proteins in cellular component, such as 'ribosome', 'endoplasmic reticulum part' and 'intracellular ribonucleoprotein complex'. In biological processes, down-regulated phosphorylated proteins were primarily enriched in catabolic process of mRNA and protein translation, such as 'nuclear-transcribed mRNA catabolic process', 'mRNA catabolic process' and 'nuclear-transcribed mRNA catabolic process, deadenylation-dependent decay'. In molecular function, 'enzyme inhibitor activity' and 'peptidase regulator activity' were enriched. In addition, in cellular components, down-regulated phosphorylated proteins that related to cytoskeleton were enriched, such as 'cytoskeleton', 'polymeric cytoskeletal fibre' and 'intermediate filament cytoskeleton' (Fig. 5).

KEGG enrichment analysis revealed that proteins that contained up-regulated phosphorylated sites were associated with 'ribosome', 'RNA transport' and 'protein export' pathways. Proteins that contained down-regulated phosphorylated sites were remarkably enriched in 12 pathways (Fig. 6), such as 'MAPK signaling pathway', 'RNA degradation', 'Oxytocin signaling pathway' and 'Calcium signaling pathway'.

Protein domain enrichment analysis revealed that 'Spen paralogue and orthologue SPOC, C-terminal' and 'Zinc finger, C2H2-like' were enriched in proteins that contained up-regulated phosphorylated sites. For proteins that contained down-regulated phosphorylated sites, 14 protein domains were enriched (Fig. 7).

Validation of changes in phosphorylated proteins level by western blot

Phosphorylation levels of ACACA, EIF4EBP1, IRS1 and JUN were tested by western blot in PL and LL. The result showed phosphorylation levels of ACACA, EIF4EBP1 and IRS1 increased and JUN decreased in PL compared with LL (Fig. 8).

Discussion

Protein phosphorylation regulated many cellular processes in eukaryotic cells by post-translational modification[10]. Protein phosphorylation revealed the effect of temperature on wheat leaf and spikelet[11] and the importance of protein phosphorylation for different chloroplast functions[12]. Protein phosphorylation had an important role in sperm quality[13] and an important connection with lactation[5, 14]. The level of phosphorylation was constantly changing in breast tissues throughout the development of the gland or different stages of lactation[3]. In addition, the level of phosphorylated proteins was detected by LC-MS/MS and TMT in PL and LL. These results contribute to the elucidation of the mechanism underlying the regulation of lactation in goat breast tissues by phosphorylation.

The production of milk was increasing after parturition and subsequently reached the maximum[15]. These phenomena were dependent on a series of factors, including somatotropin, insulin and functional protein. Nevertheless, the effect of protein phosphorylation on goat breast tissues during lactation remained unclear. Therefore, the differentially phosphorylated proteins were explored in goat breast tissues. A total of 1,938 differentially modified modification sites of 1,172 proteins were found between PL and LL. The western blot result of phosphorylation levels of ACACA, EIF4EBP1, IRS1 and JUN showed that the results of phosphoproteome were reliable and these results were consistent with this studies[16, 17]. Previous studies showed APOC3, FASN and ACACA proteins were highly correlated with the decomposition and utilisation of fat[18–20]. Moreover, the inactivation of PLIN4 could decrease fat accumulation[21]. The phosphorylation levels of mTOR, RPS6KB and STAT5B were closely related to the synthesis of milk fat and proteins[22–25]. SLC2A1 was the primary glucose transporter of glucose metabolism[26]. The effect of DFFA was closely related to apoptosis[27]. Insulin regulated glucose uptake and metabolism by binding to an insulin receptor[28], insulin receptors (IRS1 and IRS2) were necessary for insulin to function. The mTOR pathway was a key regulation pathway of lactation. PRKAA, IRS1, RPS6KB, EIF4EBP1, TSC2, FASN and ACACA were located in the mTOR pathway, previous studies showed that activation of mTOR pathway could enhance the synthesis of lactose and triglyceride[29, 30]. As expected, the result of this study showed phosphorylation levels of these proteins (FASN, ACACA, APOC3, SLC2A1, FLNA, IRS1, PLIN4 and DFFA) were changed in different stages of lactation, so we speculate that the changes of these proteins phosphorylation levels may be related to lactation.

The energy metabolism of breast tissues increased remarkably during lactation[31]. GO enrichment showed several differentially phosphorylated proteins enriched in biological processes, which were related to energy metabolism, material transport and protein translation. The results provided an overview of dynamic changes in lactation. A series of signalling pathways was enriched in PL compared with LL, such as 'Ribosome' (chx03010), 'RNA transport' (chx03013), 'Protein export' (chx03060), 'Calcium signalling pathway' (chx04020), 'Oxytocin signalling pathway' (chx04921), 'RNA degradation' (chx03018) and 'MAPK signalling pathway' (chx04010). As such, the results showed that protein translation, energy metabolism and hormone regulation were essential for lactation and these KEGG pathways might play important roles during lactation. In summary, GO and KEGG analyses provided a better understanding of the cellular components, molecular functions and biological processes of differentially phosphorylated proteins in goat mammary gland epithelial tissues and provided a reference for future research.

Conclusions

the present study was the first to sequence phosphorylated proteomics in mammary tissues of dairy goats and this study markedly increased the current understanding of post-translational modifications of proteins events that occur during the progression of lactation. The western blot result of phosphorylation levels of ACACA, EIF4EBP1, IRS1 and JUN showed that the results of phosphoproteome were reliable. FASN, ACACA, APOC3, SLC2A1, FLNA, IRS1, PLIN4 and DFFA proteins as part of the results might have potential research value in regulating goat lactation and we will study the function of these proteins in lactation in the future. So, the present study provided valuable information for the further study of the molecular mechanism of lactation in goats.

Methods

Mammary gland tissue collection and cell culture

Guanzhong dairy goats were obtained from Longxian Goat Breeding Center, in Longxian County of Shaanxi Province, China. All procedures in our animal study were approved by the Animal Care and Use Committee of the Northwest A&F University (Yangling, China) (permit number: 17-347, data:2017-10-13). Breast tissues were collected at the LL (280 days postpartum) and PL (90 days postpartum) periods from 18 healthy Guanzhong dairy goats (3 year olds) by surgery (9 breast tissues in PL and 9 breast tissues in LL). First of all, one side of the mammary gland of the dairy goat was wiped clean with alcohol, and then local anesthesia was performed on the mammary tissue. A 5-6-cm incision was made and the skin pulled back using sterile forceps, exposing the mammary tissue. 1 cm² samples were taken using a sterile scalpel blade and forceps. In order to stop any external bleeding, pressure was applied with sterile gauze to stop any external bleeding. The incision was closed with 6 to 8 surgical staples (#89063337, Appose ULC Skin Stapler, 35 wide; Henry Schein Inc., Melville, NY). After that, Keep the goat in a clean and hygienic place, the skin around the site of wound was sterilized with iodine tincture and 75% alcohol, and assign special person to take care of it. All collected tissues were washed with Rnase-free PBS and then frozen in liquid nitrogen and stored at -80 °C.

Protein extraction

The mammary gland epithelial tissues of dairy goats in PL and LL were grinded into cell powder in the presence of liquid nitrogen. The cell powder was transferred to a 5 mL centrifuge tube. Subsequently, the cell powder was added to four volumes of lysis buffer (8 M urea, 1% Protease Inhibitor Cocktail, 2 nM EDTA), followed by thrice of ultrasonic treatment on ice with a high-intensity ultrasonic processor (Scientz, Ningbo, China). The remaining debris was removed by centrifugation at 12,000 g at 4 °C for 10 min. Finally, the supernatant was collected, and the protein concentration was quantified using the BCA kit (Scientz, Ningbo, China). Proteins were extracted from 18 breast tissues of dairy goats that included nine breast tissues in PL and nine breast tissues in LL. Afterwards, proteins extracted from nine breast tissues in PL were divided into three groups. Each group was made up of three parts of protein extracted from PL breast tissues. The same method was used to construct the LL protein library.

Trypsin digestion

The protein solution was reduced with 5 mM dithiothreitol for 30 min at 56 °C and alkylated with 11 mM iodoacetamide for 15 min at room temperature in the dark. Consequently, the protein solution was digested. The protein sample was diluted by adding 100 mM triethylammonium bicarbonate (TEAB). The concentration of urea in the solution should be less than 2 M. Finally, trypsin and protein were added at 1:50 mass ratio for the first digestion overnight and at 1:100 mass ratio for the second digestion for 4 h.

TMT labelling and HPLC fractionation

The production was desalted by a Strata X C18 SPE column (Phenomenex, Torrance, USA) after trypsin digestion and vacuum drying. Afterwards, peptides were reconstituted in 0.5 M TEAB and processed using a TMT kit (Scientz, Ningbo, China). Peptides were labelled using TMT for quantitation; labelling was performed as previously described[32]. One unit of TMT reagent was thawed and reconstituted in acetonitrile. The peptide mixtures were incubated for 2 h at room temperature, pooled, desalted and dried by vacuum centrifugation. The tryptic peptides were divided into segments using a Thermo Betasil C18 column (5 µm particles, 10 mm ID, 250 mm length) by high pH reversed-phase HPLC. In summary, peptides were separated into 60 fractions after more than 60 min of gradient treatment with 8%–32% acetonitrile (pH 9.0). Subsequently, the peptides were combined into eight fractions and dried by vacuum centrifuging. Reactions were quenched using 8 µL of 11% lysine following the manufacturer's recommendations. Finally, 10% trifluoroacetic acid (TFA, Sigma–Aldrich) was added into the peptide solutions. The volume ratio of the peptide solution to TFA was 1:10, and the mixture was pooled, desalted and dried by vacuum centrifugation.

Affinity enrichment

The mixtures were first incubated with immobilised metal affinity chromatography (IMAC) microsphere suspensions with vibration in loading buffer (50% acetonitrile/6% TFA). Phosphopeptide-rich IMAC microspheres were collected by centrifugation. Afterwards, the supernatant was removed. The IMAC

microspheres were washed with 50% acetonitrile/6% TFA and 30% acetonitrile/0.1% TFA to remove nonspecifically adsorbed peptides. To elute the enriched phosphopeptides from the IMAC microspheres, an elution buffer containing 10% NH₄OH was added, and the enriched phosphopeptides were eluted with vibration. The supernatant containing phosphopeptides was collected for LC–MS/MS analysis after lyophilisation.

LC–MS/MS analysis

The tryptic peptides were dissolved in 0.1% formic acid (solvent A), directly loaded onto a homemade reversed-phase analytical column (15 cm length, 75 µm i.d.). The gradient consisted of solvent B (0.1% formic acid in 98% acetonitrile), which increased from 6% to 23% over 26 min, 23% to 35% in 8 min and climbing to 80% in 3 min, followed by holding at 80% for the last 3 min, all at a constant flow rate of 400 nL/min on an EASY-Nlc 1,000 ultra-performance liquid chromatography (UPLC) system.

Peptides were characterised using tandem mass spectrometry (MS/MS) in Q Exactive™ Plus (Thermo) coupled online to the UPLC after the peptides were subjected to NSI source. The electrospray voltage applied was 2.0 Kv. The m/z scan was 350 to 1,800 for full scan, and intact peptides were detected in the Orbitrap at a resolution of 70,000. Using a normalization collision energy setting of 28, the fragments were detected in the Orbitrap at a resolution of 17,500 for the selected MS/MS of peptides. A data-dependent procedure was alternated between one MS scan followed by 20 MS/MS scans with a 15.0 s dynamic exclusion. The automatic gain control was set at 5E4. The fixed first mass was set at 100 m/z.

Database search

Maxquant search engine (V.1.5.2.8) was used to process the resulting MS/MS data. The UniProt Ovis aries (27472 sequences) concatenated with a decoy database that was used for the tandem mass spectra search. The search parameters were as follows: 6-plex TMT, the minimum length of the peptides was set at 7 amino acid residues and the maximum modification number of the peptides was set at 5; fixed modification (carbamidomethylation of cysteine residues); variable modification (protein N-term acetylation); and oxidation of methionine residues and phosphorylation of serine, threonine and tyrosine residues, thereby allowing two missing cleavages by cleavage enzyme trypsin/P. The mass error was set at 20 ppm in the first search and 5 ppm in the primary search, and the fragment ions of mass tolerance were set at 0.02 Da. The minimum score for modified peptides was set at > 40, and a false discovery rate was set at < 1%.

Bioinformatics analysis

Gene Ontology (GO) annotation data were obtained from UniProt GoA database. Proteins were divided into three categories by GO annotation, namely, a biological process, cellular compartment and molecular function. The GO with a corrected *P* value < 0.05 was considered significant. InterProScan (<http://www.ebi.ac.uk/interpro/>) was used to detect the enrichment of functional domains of differentially expressed proteins compared with all identified proteins. Protein domains with a corrected *P*

value < 0.05 were considered significant. The KEGG database (https://www.genome.jp/kegg/tool/map_pathway2.html) was used to identify enriched pathways. The pathway with a corrected P value < 0.05 was considered significant. Based on the KEGG website, these pathways were classified into hierarchical categories. Fisher's exact test was used to examine the enrichment of the differentially phosphorylation protein against all identified phosphorylation proteins. Wolfpsort, a subcellular localisation predication wolf, was used to predict subcellular localisation. Soft motif-x was used to analyse the sequence model constituted with amino acids in specific positions of modify-21-mers (10 amino acids upstream and downstream of the site) in all protein sequences. In addition, all database protein sequences were used as background database parameter, as well as other parameters with default.

Enrichment-based clustering

Hierarchical clustering was based on the functional classification of different proteins. Categories that were at least enriched in one of the clusters with $P < 0.05$ were filtered after collating all the categories and their P values. This filtered P value matrix was transformed by the function $x = -\log_{10}(P \text{ value})$. Finally, these x values were z-transformed for each functional category. These z scores were then clustered by one-way hierarchical clustering (Euclidean distance and average linkage clustering) in Genesis. Cluster membership was visualised by a heat map using the "heatmap.2" function from the "gplots" R-package.

Western blot

Approximately 25 μg of protein which extracted from goat mammary gland epithelial tissues was transferred onto polyvinylidene difluoride membrane (PVDF, Merck Millipore, MA, USA). The polyvinylidene difluoride membrane was immersed in 10% skimmed milk powder and diluted with Tris-buffered saline inclusive of 0.1% Tween 20 (pH 7.6) for 2.5 h at room temperature. The membrane was immersed in corresponding primary antibodies overnight at 4 °C (Table 1). In the next step, the membrane was incubated in suitable HRP-conjugated secondary antibodies against mouse, rabbit at 4 °C for 2 h. Proteins were visualised using ECL prime western blotting detection reagent (Amersham, GE Healthcare Lifesciences, Swenden) by gel documentation system (Biospectrum 410, UVP). Proteins were quantified by the Quantity One program (Bio-Rad, California, USA).

Statistics

Each experiment was repeated at least three times. All the data were processed by SPSS 19.0 (Beijing, China). The results were shown as means \pm SE (standard error), and the differences were compared by one-way ANOVA (** $P < 0.01$, * $P < 0.05$).

Abbreviations

FASN: fatty acid synthase; ACACA: acetyl-CoA carboxylase 1 isoform X3; APOC3: apolipoprotein C-III; SLC2A1: solute carrier family 2, facilitated glucose transporter member 1; mTOR: serine/threonine-protein

kinase mTOR; RPS6KB: ribosomal protein S6 kinase beta-1 isoform X1; STAT5B: signal transducer and activator of transcription 5B isoform X2; PLIN4: perilipin-4 isoform X2; DFFA: DNA fragmentation factor subunit alpha; IRS1: insulin receptor substrate 1; PRKAA: 5'-AMP-activated protein kinase catalytic subunit alpha-2; RPS6KB: ribosomal protein S6 kinase beta-1 isoform X1; EIF4EBP1: eukaryotic translation initiation factor 4E-binding protein 1; TSC2: tuberin; JUN: transcription factor AP-1.

Declarations

Acknowledgements

The authors would like to thank Yuxuan Song for excellent assistance in editing the manuscript.

Author's contributions

CZ analysed the data and drafted the manuscript; CZ, YJ, JZ, YH and QD performed the statistical analysis; HY, WL, FL and ZW performed the experiments; XA conceived and coordinated the study. All authors read and approved the final manuscript.

Funding

This study was supported by the National Natural Science Foundation of China (31601925), China Postdoctoral Science Foundation (2016T90954 and 2014M552498) and Shaanxi Science and Technology Innovation Project Plan (2017ZDXM-NY-081 and 2018ZDCXL-NY-01-04). The funding bodies played no role in the design of the study and collection, analysis, and interpretation of data and in writing the manuscript.

Availability of data and materials

Not applicable.

Ethics approval and consent to participate

Not applicable.

Consent for publication

Not applicable.

Competing interests

The authors declare that they have no competing interests.

Author details

References

1. Humphrey SJ, Yang G, Yang P, Fazakerley DJ, Stockli J, Yang JY, James DE. Dynamic adipocyte phosphoproteome reveals that Akt directly regulates mTORC2. *Cell Metabol.* 2013;17(6):1009–20.
2. Areces LB, Matafora V, Bachi A. Analysis of protein phosphorylation by mass spectrometry. *Eur J Mass Spectrom (Chichester Engl).* 2004;10(3):383–92.
3. Toerien CA, Trout DR, Cant JP. Nutritional stimulation of milk protein yield of cows is associated with changes in phosphorylation of mammary eukaryotic initiation factor 2 and ribosomal s6 kinase 1. *J Nutr.* 2010;140(2):285–92.
4. Jones FE, Welte T, Fu XY, Stern DF. ErbB4 signaling in the mammary gland is required for lobuloalveolar development and Stat5 activation during lactation. *J Cell Biol.* 1999;147(1):77–88.
5. Lin Y, Duan X, Lv H, Yang Y, Liu Y, Gao X, Hou X. The effects of L-type amino acid transporter 1 on milk protein synthesis in mammary glands of dairy cows. *J Dairy Sci.* 2018;101(2):1687–96.
6. Li H, Liu X, Wang Z, Lin X, Yan Z, Cao Q, Zhao M, Shi K. MEN1/Menin regulates milk protein synthesis through mTOR signaling in mammary epithelial cells. *Sci Rep.* 2017;7(1):5479.
7. Gall L, Le Gal F, De Smedt V. Protein phosphorylation patterns during in vitro maturation of the goat oocyte. *Mol Reprod Dev.* 1993;36(4):500–6.
8. Kuzmanov U, Guo H, Buchsbaum D, Cosme J, Abbasi C, Isserlin R, Sharma P, Gramolini AO, Emili A. Global phosphoproteomic profiling reveals perturbed signaling in a mouse model of dilated cardiomyopathy. *Proc Natl Acad Sci U S A.* 2016;113(44):12592–7.
9. Wilson-Grady JT, Haas W, Gygi SP. Quantitative comparison of the fasted and re-fed mouse liver phosphoproteomes using lower pH reductive dimethylation. *Methods.* 2013;61(3):277–86.
10. Preisinger C, von Kriegsheim A, Matallanas D, Kolch W. Proteomics and phosphoproteomics for the mapping of cellular signalling networks. *Proteomics.* 2008;8(21):4402–15.
11. Vu LD, Zhu T, Verstraeten I, van de Cotte B, Gevaert K, De Smet I. Temperature-induced changes in the wheat phosphoproteome reveal temperature-regulated interconversion of phosphoforms. *J Exp Bot.* 2018;69(19):4609–24.
12. Reiland S, Messerli G, Baerenfaller K, Gerrits B, Endler A, Grossmann J, Gruissem W, Baginsky S. Large-scale Arabidopsis phosphoproteome profiling reveals novel chloroplast kinase substrates and phosphorylation networks. *Plant physiology.* 2009;150(2):889–903.
13. Huang Z, Danshina PV, Mohr K, Qu W, Goodson SG, O'Connell TM, O'Brien DA. Sperm function, protein phosphorylation, and metabolism differ in mice lacking successive sperm-specific glycolytic enzymes. *Biol Reprod.* 2017;97(4):586–97.
14. Liu J, Wang Y, Li D, Wang Y, Li M, Chen C, Fang X, Chen H, Zhang C. Milk protein synthesis is regulated by T1R1/T1R3, a G protein-coupled taste receptor, through the mTOR pathway in the

- mouse mammary gland. *Molecular nutrition & food research*. 2017, 61(9).
15. Wiltbank MC, Baez GM, Garcia-Guerra A, Toledo MZ, Monteiro PL, Melo LF, Ochoa JC, Santos JE, Sartori R. Pivotal periods for pregnancy loss during the first trimester of gestation in lactating dairy cows. *Theriogenology*. 2016;86(1):239–53.
 16. Zhu C, Jiang Y, Zhu J, He Y, Yin H, Duan Q, Zhang L, Cao B, An X. CircRNA8220 Sponges MiR-8516 to Regulate Cell Viability and Milk Synthesis via Ras/MEK/ERK and PI3K/AKT/mTOR Pathways in Goat Mammary Epithelial Cells. *Animals: an open access journal from MDPI*. 2020, 10(8).
 17. Chen K, Hou J, Song Y, Zhang X, Liu Y, Zhang G, Wen K, Ma H, Li G, Cao B, et al. Chi-miR-3031 regulates beta-casein via the PI3K/AKT-mTOR signaling pathway in goat mammary epithelial cells (GMECs). *BMC Vet Res*. 2018;14(1):369.
 18. Russo GT, Meigs JB, Cupples LA, Demissie S, Otvos JD, Wilson PW, Lahoz C, Cucinotta D, Couture P, Mallory T, et al. Association of the Sst-I polymorphism at the APOC3 gene locus with variations in lipid levels, lipoprotein subclass profiles and coronary heart disease risk: the Framingham offspring study. *Atherosclerosis*. 2001;158(1):173–81.
 19. Travers MT, Cambot M, Kennedy HT, Lenoir GM, Barber MC, Joulin V. Asymmetric expression of transcripts derived from the shared promoter between the divergently oriented ACACA and TADA2L genes. *Genomics*. 2005;85(1):71–84.
 20. Hao J, Zhu L, Zhao S, Liu S, Liu Q, Duan H. PTEN ameliorates high glucose-induced lipid deposits through regulating SREBP-1/FASN/ACC pathway in renal proximal tubular cells. *Experimental cell research*. 2011;317(11):1629–39.
 21. Chen W, Chang B, Wu X, Li L, Sleeman M, Chan L. Inactivation of Plin4 downregulates Plin5 and reduces cardiac lipid accumulation in mice. *American journal of physiology Endocrinology metabolism*. 2013;304(7):E770–9.
 22. Akers RM. Major advances associated with hormone and growth factor regulation of mammary growth and lactation in dairy cows. *J Dairy Sci*. 2006;89(4):1222–34.
 23. Bian CX, Shi Z, Meng Q, Jiang Y, Liu LZ, Jiang BH. P70S6K 1 regulation of angiogenesis through VEGF and HIF-1alpha expression. *Biochem Biophys Res Commun*. 2010;398(3):395–9.
 24. Yang X, Yang C, Farberman A, Rideout TC, de Lange CF, France J, Fan MZ. The mammalian target of rapamycin-signaling pathway in regulating metabolism and growth. *J Anim Sci*. 2008;86(14 Suppl):E36–50.
 25. Reichenstein M, Rauner G, Barash I. Conditional repression of STAT5 expression during lactation reveals its exclusive roles in mammary gland morphology, milk-protein gene expression, and neonate growth. *Mol Reprod Dev*. 2011;78(8):585–96.
 26. Deng D, Sun P, Yan C, Ke M, Jiang X, Xiong L, Ren W, Hirata K, Yamamoto M, Fan S, et al. Molecular basis of ligand recognition and transport by glucose transporters. *Nature*. 2015;526(7573):391–6.
 27. Fawzy MS, Toraih EA, Ibrahiem A, Abdeldayem H, Mohamed AO, Abdel-Daim MM. Evaluation of miRNA-196a2 and apoptosis-related target genes: ANXA1, DFFA and PDCD4 expression in gastrointestinal cancer patients: A pilot study. *PLoS One*. 2017;12(11):e0187310.

28. Li Y, Soos TJ, Li X, Wu J, Degennaro M, Sun X, Littman DR, Birnbaum MJ, Polakiewicz RD. Protein kinase C Theta inhibits insulin signaling by phosphorylating IRS1 at Ser(1101). *J Biol Chem.* 2004;279(44):45304–7.
29. Wang L, Lin Y, Bian Y, Liu L, Shao L, Lin L, Qu B, Zhao F, Gao X, Li Q. Leucyl-tRNA synthetase regulates lactation and cell proliferation via mTOR signaling in dairy cow mammary epithelial cells. *Int J Mol Sci.* 2014;15(4):5952–69.
30. Zhu C, Wang L, Zhu J, Jiang Y, Du X, Duan Q, Yin H, Huang X, Song Y, Cao B, et al. OGR1 negatively regulates β -casein and triglyceride synthesis and cell proliferation via the PI3K/AKT/mTOR signaling pathway in goat mammary epithelial cells. *Animal biotechnology.* 2020:1–10.
31. Gross JJ, Schwarz FJ, Eder K, van Dorland HA, Bruckmaier RM. Liver fat content and lipid metabolism in dairy cows during early lactation and during a mid-lactation feed restriction. *J Dairy Sci.* 2013;96(8):5008–17.
32. Plubell DL, Wilmarth PA, Zhao Y, Fenton AM, Minnier J, Reddy AP, Klimek J, Yang X, David LL, Pamir N. Extended Multiplexing of Tandem Mass Tags (TMT) Labeling Reveals Age and High Fat Diet Specific Proteome Changes in Mouse Epididymal Adipose Tissue. *Molecular & cellular proteomics: MCP.* 2017, 16(5):873–890.

Tables

Table 1. The antibody used in the present study.

Name	Manufacturer	Product number
β -Actin	[Beyotime, Shanghai, China]	AA128
JUN	Signalway Antibody, College Park, USA	GTX82231
p-JUN (Ser63)	Signalway Antibody, College Park, USA	CY5418
ACACA	Signalway Antibody, College Park, USA	CY5854
p-ACACA(Ser80)	Signalway Antibody, College Park, USA	CY5168
EIF4EBP1	Signalway Antibody, College Park, USA	CY5277
p- EIF4EBP1(Thr46)	Signalway Antibody, College Park, USA	A0208
IRS1	Abcam, UK	A0216
p-IRS1(Ser312)	Signalway Antibody, College Park, USA	
HRP-labeled Goat Anti-Rabbit IgG (H + L)	Beyotime, Shanghai, China	
HRP-labeled Goat Anti-Mouse IgG (H + L)	Beyotime, Shanghai, China	

Figures

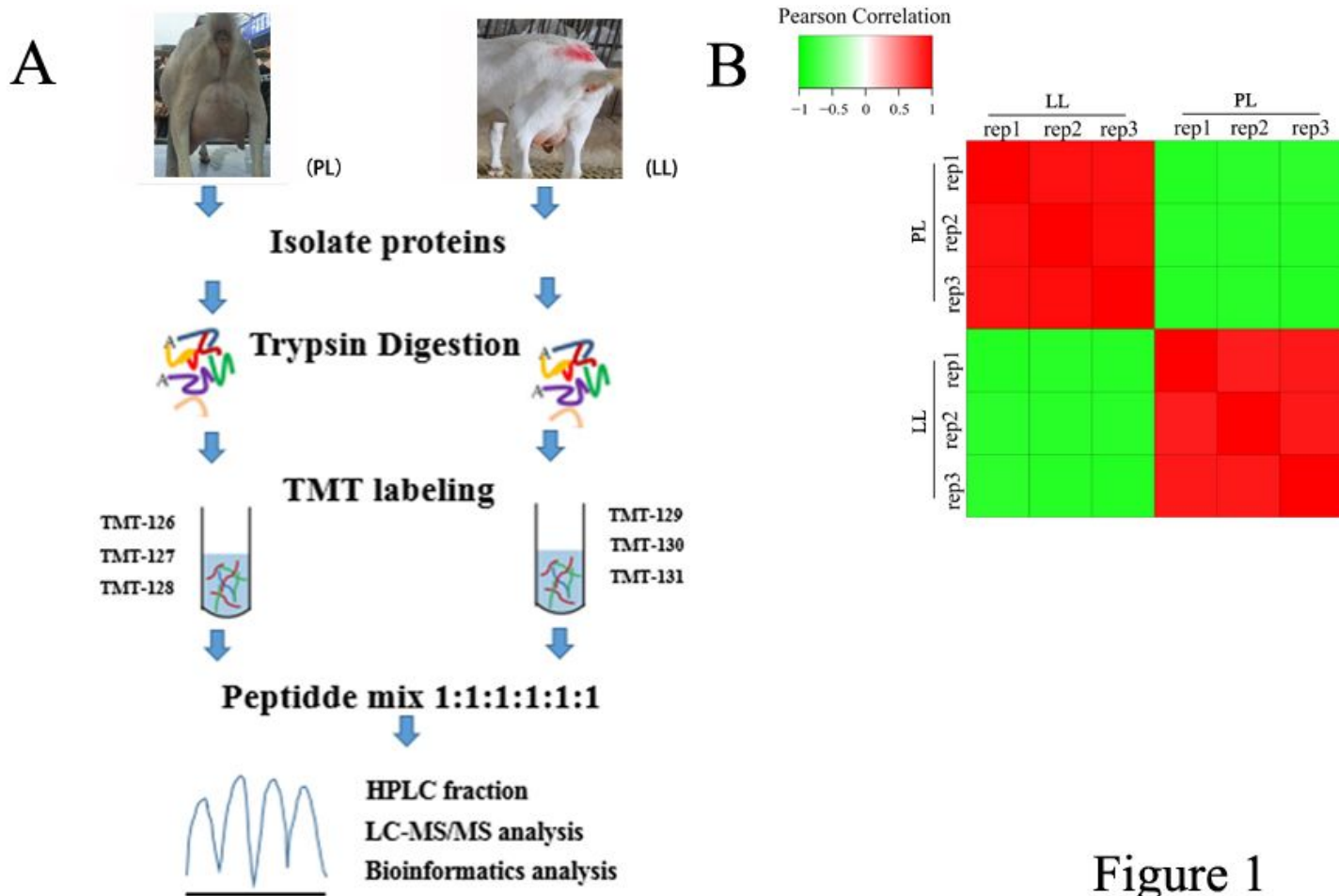


Figure 1

Figure 1

Experimental strategy for quantitative proteome analysis and quality control validation of MS data. A The workflow of the study; proteins were extracted in three biological replicates for each sample group. B Pearson's Correlation Coefficient of protein quantitation.

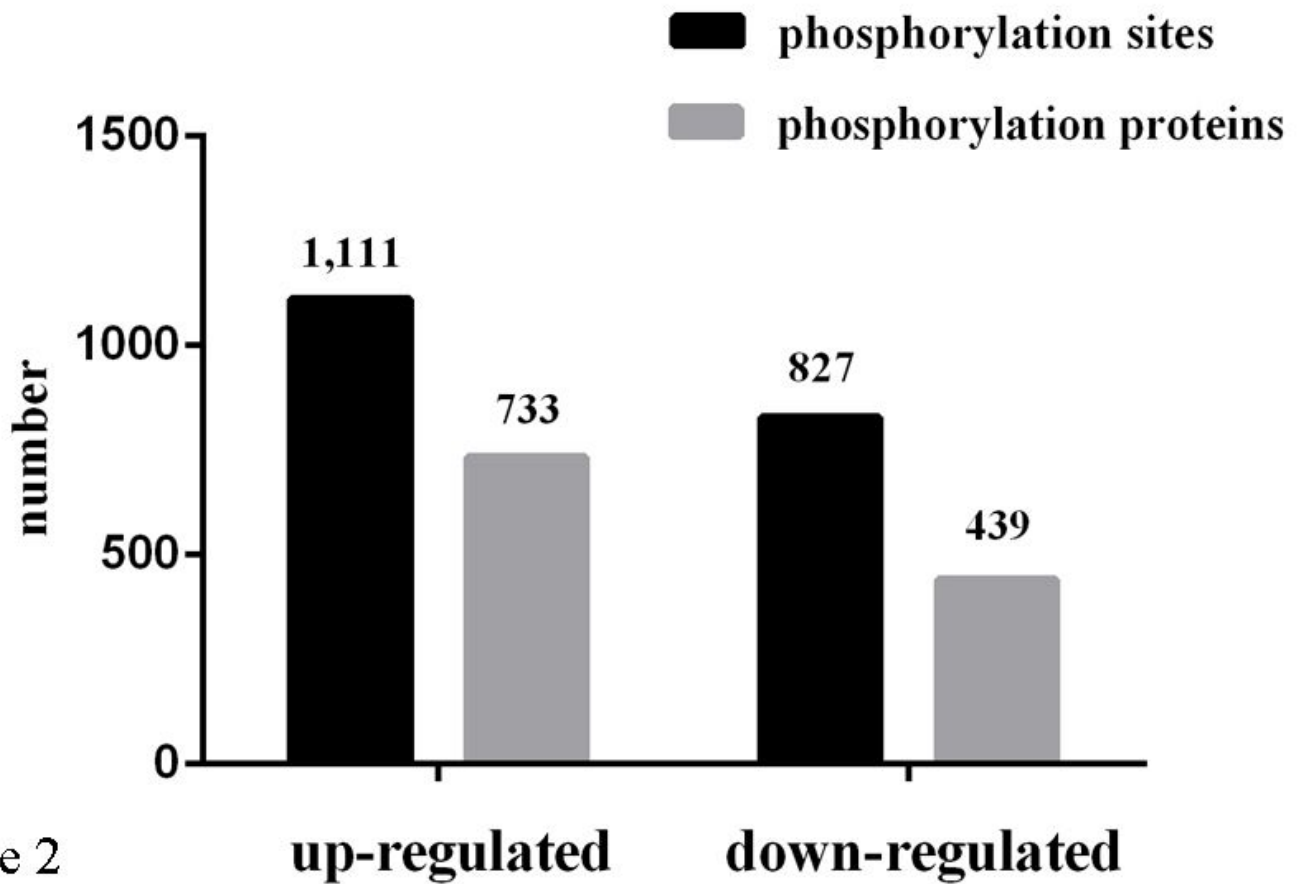


Figure 2

The numbers of differentially modified modification sites and phosphorylated proteins.

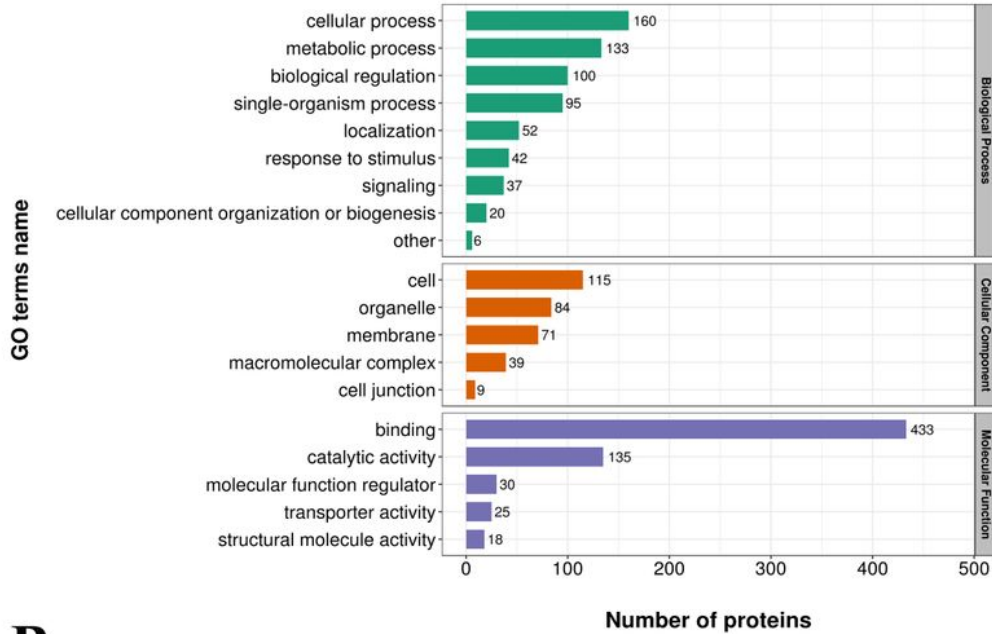
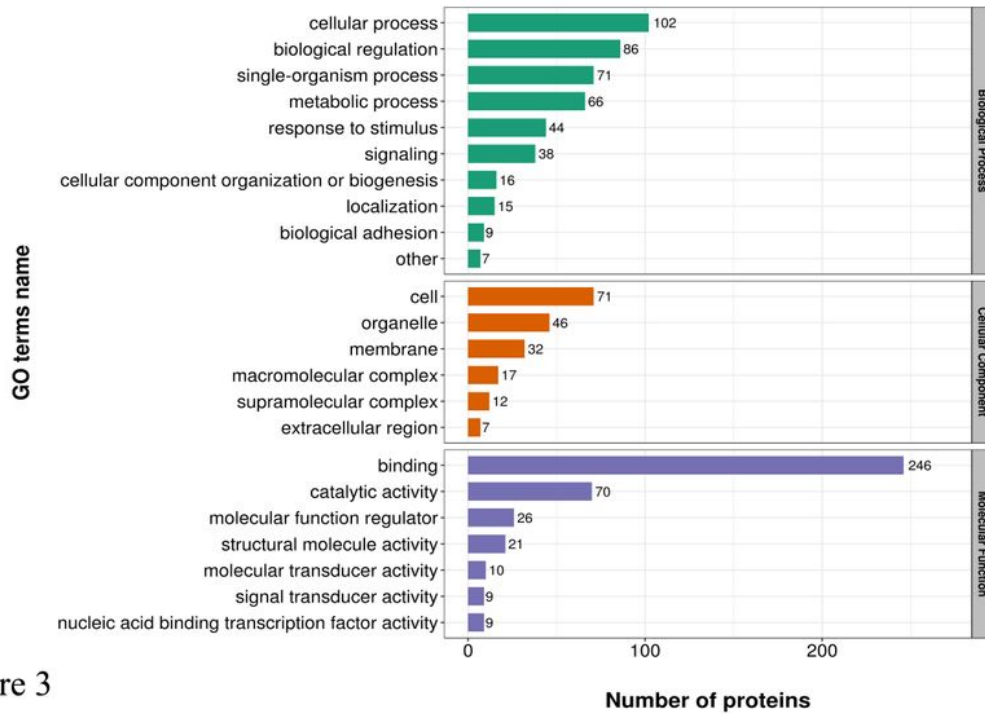
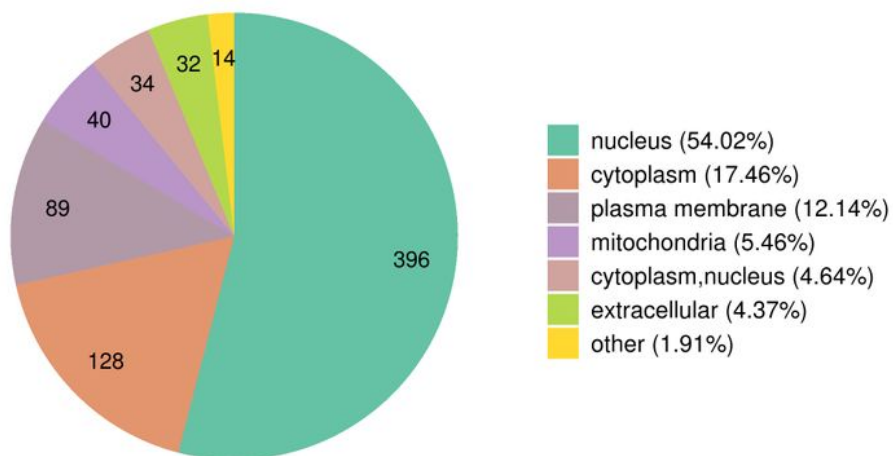
A**B**

Figure 3

Figure 3

Distribution of the up-regulated phosphorylated proteins (A: biological process, B: cellular component, C: molecular function) and down-regulated phosphorylated proteins (D: biological process, E: cellular component, F: molecular function) with GO annotation.

A



B

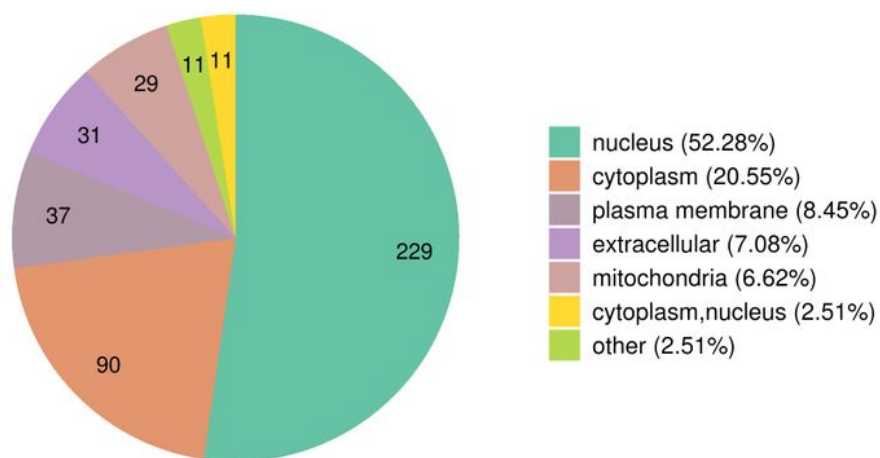


Figure 4

Figure 4

Subcellular locations of up-regulated phosphorylated proteins (A) and down-regulated phosphorylated proteins (B).

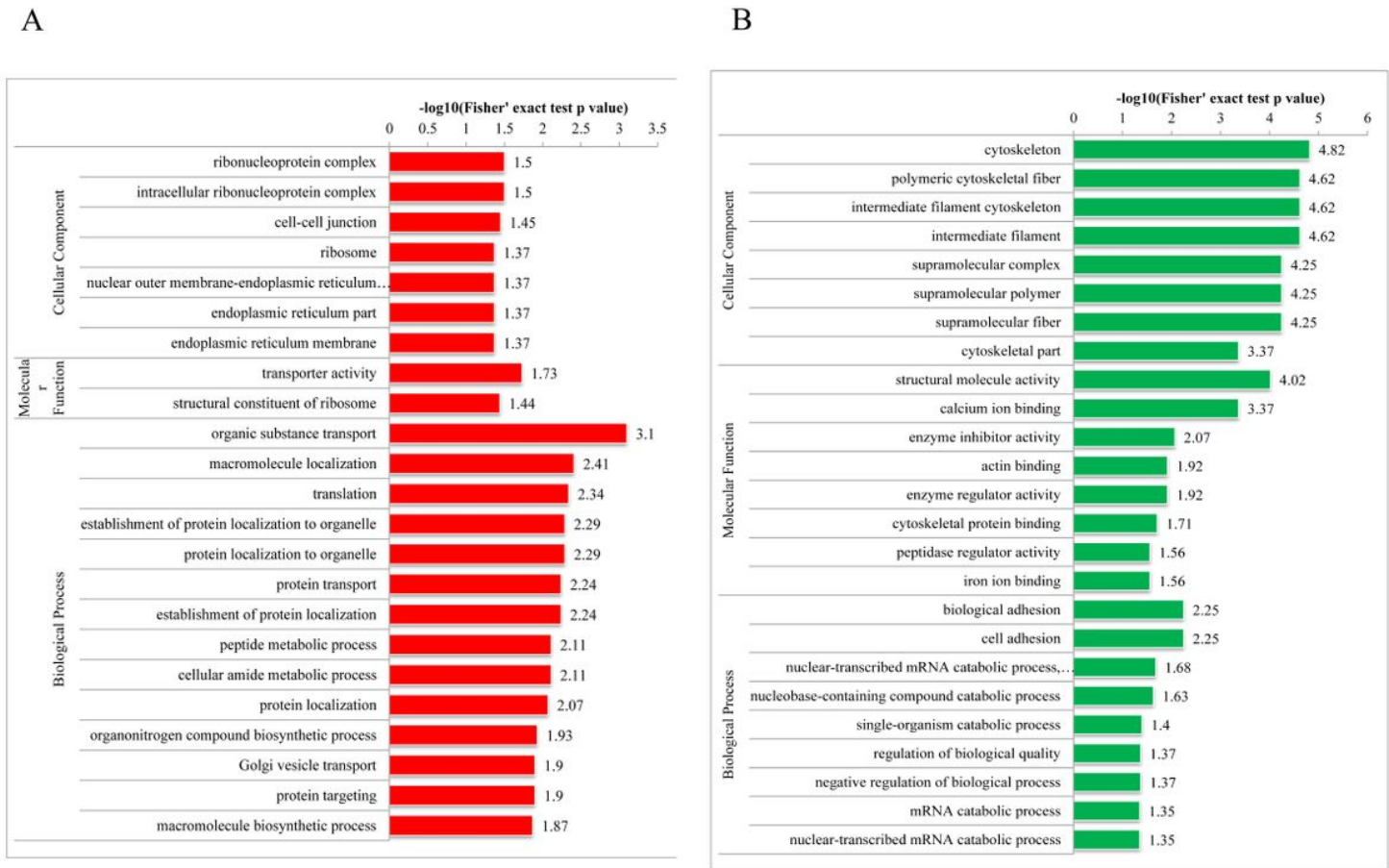
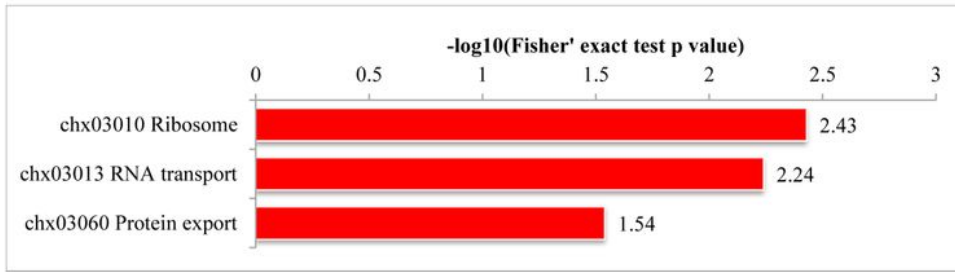


Figure 5

Remarkably enriched GO terms of the up-regulated phosphorylated proteins (A) and down-regulated phosphorylated proteins (B) concerning cellular component, molecular function and biological process.

A



B

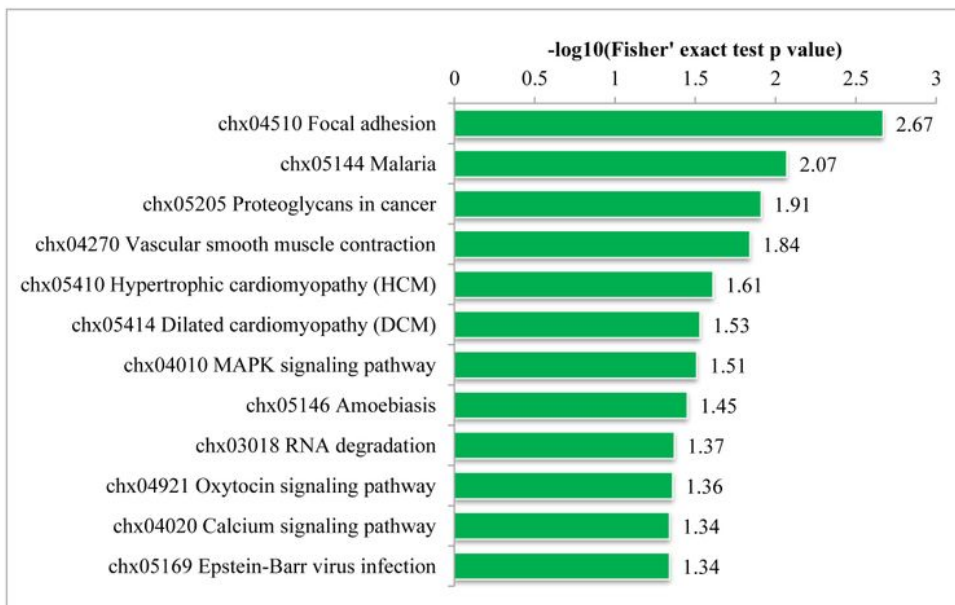
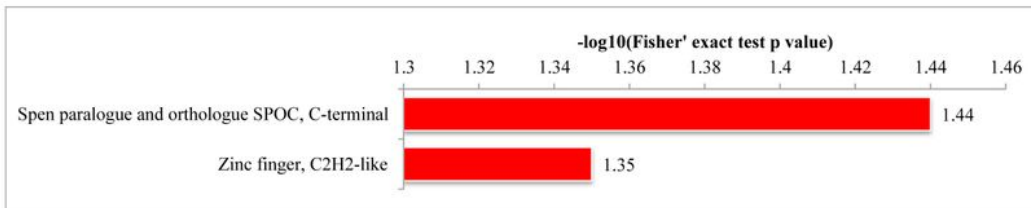


Figure 6

KEGG enrichment analysis of the up-regulated phosphorylated proteins (A) and down-regulated phosphorylated proteins (B).

A



B

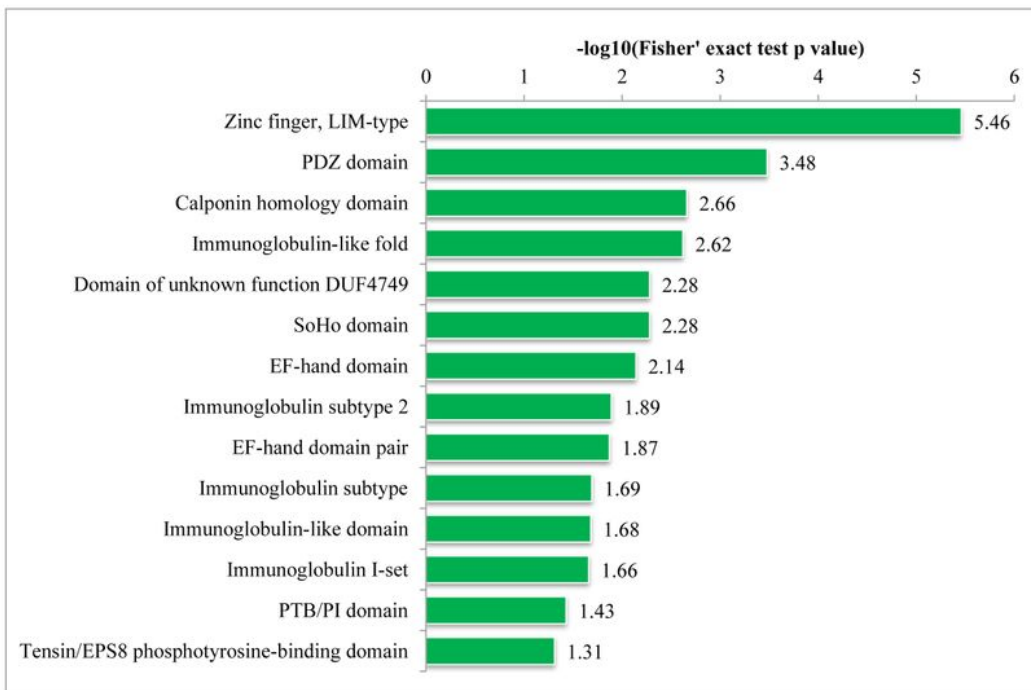


Figure 7

Domain enrichment analysis of the up-regulated phosphorylated proteins (A) and down-regulated phosphorylated proteins (B).

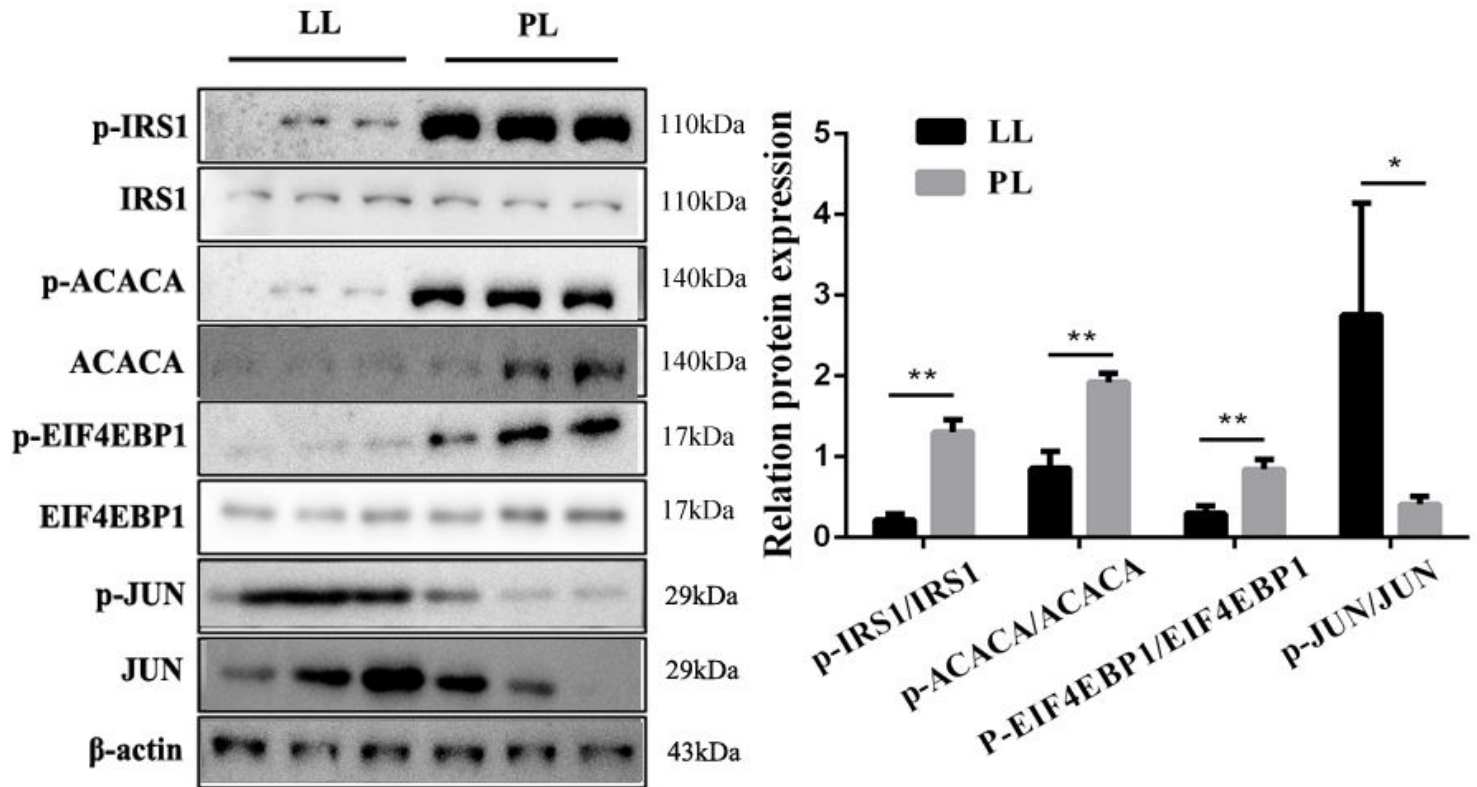


Figure 8

Protein levels of p-IRS1(full-length blots/gels are presented in Additional figure S3), IRS1(full-length blots/gels are presented in Additional figure S4), p-ACACA(full-length blots/gels are presented in Additional figure S5), ACACA(full-length blots/gels are presented in Additional figure S6), p-EIF4EBP1(full-length blots/gels are presented in Additional figure S7), EIF4EBP1(full-length blots/gels are presented in Additional figure S8), p-JUN(full-length blots/gels are presented in Additional figure S9), JUN(full-length blots/gels are presented in Additional figure S10) in PL and LL were detected by western blot. Full-length blots/gels of β -actin are presented in Additional figure S11.

Supplementary Files

This is a list of supplementary files associated with this preprint. Click to download.

- [figureS1.jpg](#)
- [supplement2.jpg](#)
- [Actin.jpg](#)
- [JUN.jpg](#)

- PJUN.jpg
- EIF4EBP1.jpg
- PEIF4EBP1.jpg
- ACACA.jpg
- PACACA.jpg
- IRS1.jpg
- PIRS1.jpg
- SupportingInformationtables5.xlsx
- SupportingInformationtables4.xlsx
- SupportingInformationtables3.xlsx
- SupportingInformationtables2.xlsx
- SupportingInformationtables1.xlsx